

TEMPORAL AND SPATIAL DISTRIBUTION OF SUSPENDED SEDIMENT CONCENTRATION ABOVE RIPPLED SEA BED INDUCED BY WAVES

Alireza Ahmari¹ and Hocine Oumeraci²

ABSTRACT

Selected results of the analysis of the measurements of the near bed suspended sediment distribution in time and space around steep ripples are reported. A comprehensive series of laboratory measurements were performed in the Large Wave Flume (GWK) to examine the characteristics of the sediment dynamics in the near sea bed regions under controlled large scale laboratory conditions. To represent the sea bed, medium sand was used, which was covered with 3-dimensional mega ripples superimposed with 2-dimensional steep ripples at the beginning of the test runs. The use of Multi Frequency Acoustic Backscatter System (ABS) provided a high accuracy level of sediment concentration measurement both temporarily and spatially.

1. INTRODUCTION

Above sea beds covered by steep ripples, the process of sediment entrainment and suspended sediment dynamics around the ripples induced by surface waves are likely well organised. Due to the high temporal and spatial variation of the suspended sediment event in the near bed regions, which is the consequence of the interaction between the hydrodynamic forcing (waves, currents) and the sea bed morphology, particularly if the sea bed is rippled, a high temporal accuracy of the suspended sediment measurement in the near shore zone is crucial to substantially improve the understanding of all processes involved and to come up with more reliable prediction formulae. In this context, a new generation of the measurement devices (acoustic backscattering system, optical technique, laser) have been used recently to capture more details of the temporal entrainment of the sediment particles due to the intrawave processes at the sandy sea bottom. However, these experiments could not substantially contribute to provide an entire picture of the suspended concentration feature above the sea bed under different wave induced near bed flow regimes and sea bed conditions, including the distribution in the near sea bed layer induced by intrawave oscillatory flow above different bed forms. To overcome this problem, a new set of large scale laboratory measurements were carried out recently in the Large Wave Flume (GWK) in Hannover. The observations provided a detailed description of the suspended sediment dynamics near the sea bed in the case of rippled sea bed with sufficient accuracy both temporarily and spatially. Selected results are analysed in this paper exemplarily to illustrate the processes associated with the generation of the lee vortices and their shedding around the steep ripples.

¹ Dipl.-Ing., Forschungszentrum Küste (FZK), Merkurstraße 11, 30419 Hannover, ahmari@fzk-nth.de

² Prof. Dr.-Ing., Leichtweiß-Institut, Beethovenstraße 51a, 38106 Braunschweig, h.oumeraci@tu-bs.de

2. MOTIVATION AND BACKGROUND

Several previous studies (Nielsen, 1992; Thorne, et al., 2009,2003; Davies and Li, 1997; Ribberink and Al-Salem, 1994; Ahmari and Oumeraci, 2008, 2009, 2010) have shown that the flow separation and vortex generation due to the oscillatory flow at the ripple crest influences significantly the mechanism of the sediment entrainment and suspension close to the sea bed. Furthermore, the shape of the ripples contributes to the prevailing flow structure in the wave bottom boundary layer. Taking into account that the ripples themselves are

a product of the local sediment transport, it can be concluded that the sediment transport event depends upon three interacting components namely the mobile sediment characteristics, the forcing hydrodynamics and the bed forms, which interrelate each other in complex ways (Thorne et al. 2003). This triad is illustrated in Figure 1. According to the theoretical analysis of Blondeaux and Vittori (1991) and some prediction vortex models (Hansen et al. 1994; Malarkey and Davies, 2002), the process of vortex generation can schematically be described as follows (see Figure 2): Figure 2-a shows the moment of the flow separation at the crest of a steep ripple, which is followed by the generation of a lee-wake vortex, V1, at around the maximum wave induced flow velocity. Figures 2-c and b illustrate how the vortex V1 grows and becomes detached from the sea bed surface during the rest positive wave half cycle. When the flow reverses, immediately after the zero-down crossing on the wave induced flow velocity profile, vortex V2 is formed at the opposite side of the ripple and at the same time, the vortex V1 is advected over the ripple crest (Figure 2-d). Figures 2-e and f show the growth and the detachment of V2 and its movement over the ripple crest beneath the next flow reversal. Finally, Figures 2-e and f show the off-shore shedding event of vortex V1 under the rest of the wave cycle, which indicates the off-shore direction of the total net suspended sediment transport above steep ripples.

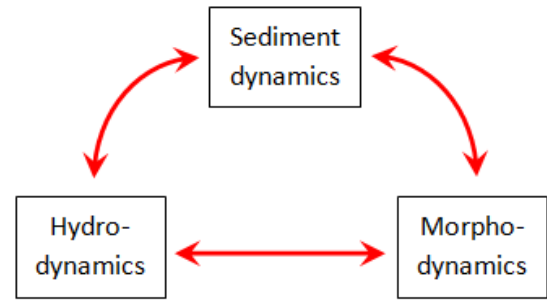


Figure 1: Sediment triad showing the inter-action between sea bed, forcing hydrodynamics and sediment dynamics

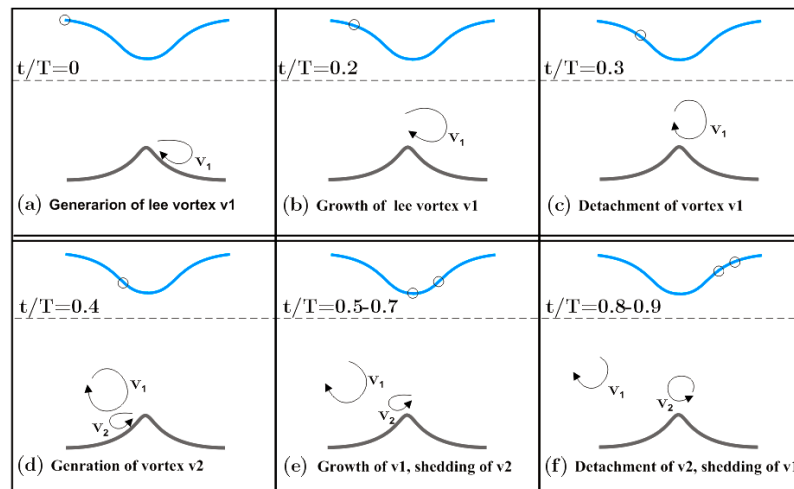


Figure 2: Vortex shedding above a steeply rippled bed (Modified from Thorne at al., 2003). V1 and V2 are lee side vortices due to flow separation at ripple crest under positively and negatively directed flow, respectively.

3. LARGE WAVE FLUME EXPERIMENTS

The experiments aiming at the determination of the suspended sediment dynamics were carried out in the Large Wave Flume (GWK) of the Coastal Research Centre (FZK) in Hannover, Germany. A sand layer ($d_{50}=0.242$ mm and the non-uniformity factor of $U = d_{60}/d_{10} = 2.24$) with the thickness of about 0.82 m was used to represent the sea bottom. The initial water depth above the sandy bottom was 3.18 m. The tests were conducted with different wave types: Regular waves ($H = 0.8, 1.0$ and 1.2 m, $T=5$ s) and irregular waves using JONSWAP-spectra ($H_s = 0.8, 1.0$ and 1.2 m with $\gamma = 1.0$ to 10.0 and $T_p = 5$ s). The two components of the wave induced flow velocity (u and w) were measured using two Electromagnetic Current Meters (ECMs) at two levels of 0.25 m and 0.45 m above the sea bottom. The measurements of the free water surface elevation were performed simultaneously using a wave gauge located at the measuring station (111.45 m from the wave paddle). Suspended sand concentrations were comparatively measured by means of an acoustical device (ABS), an optical device (Optical Turbidity Meter) and a mechanical device (TSS).

4. OBSERVATIONS

Figure 3 show a time window of suspended sediment entrainment around a steep vortex ripple ($\eta_r/\lambda_r = 0.12$) and the distribution of the suspended sediment concentration higher up into the water column under non-breaking weakly asymmetric regular waves (test conditions: $H=1.0$ m, $T=5$ s, $h/L=0.125$). The suspended concentrations at different locations of the bed evolution time series beneath ABS were combined to generate the images. Figure 3 shows that the sediment entrainment event is more significant at the lee sides of the ripple than at the ripple crest. This clearly indicates that the prior entrainment process over the steep ripples is the vortex formation process, which occurs at the ripple flanks just after the flow separation at the ripple crest.

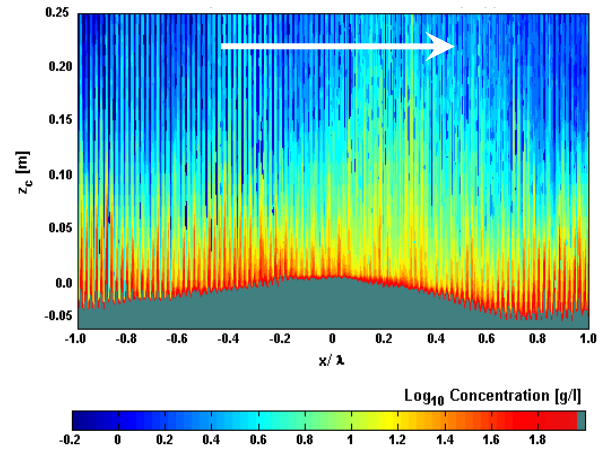


Figure 3: Suspended Sediment Concentration (SSC) above a steep ripple beneath non breaking weakly asymmetric regular waves (Test conditions: $H=1.0$ m; $T=5$ s, $h=3.18$ m). The arrowhead shows the direction of the wave propagation. The colours in the contour plot are defined in the colour bar as “Log₁₀ Concentration in g/l”.

4.1 COMPARATIVE ANALYSIS OF CONCENTRATION PROFILES FROM DIFFERENT MEASURING TECHNIQUES

Figure 4-a shows the time and horizontally averaged vertical concentration profiles under regular waves ($H=1.2$ m; $T=5$ s; $h=3.18$ m) measured by means of the Transverse Suction System (TSS) and calculated from Optical Turbidity Meter and ABS- measurement data set (ABS-measurements: closed white circles; Turbidity meter measurements: closed red circles and TSS-measurements: closed triangles). As can be seen here, ABS provides a vertical profile of the suspended concentrations above the sea bed over a defined vertical operating range up to the transducer head. The concentrations measured by Optical Turbidity meters

(red closed circles) were averaged with durations of about 20 minutes during the test runs. The TSS-measurements (black Triangles) were performed over a time period of about 20 minutes during each test. A good agreement of the time- and bed-averaged concentration measurement can be observed between the ABS- and the optical concentrations measured by Optical Turbidity Meter and the measured values by means of the Transverse Suction System (TSS). Figure 4-b shows a comparison between the “acoustic” concentrations (C_{ABS}) and the pump sampled concentrations (C_{TSS}) conducted during 37 test runs at different heights above the sand bed beneath regular and irregular waves ($H_s, H=0.8, 1.0, 1.2$ m; $T, T_p=5$ s; $\gamma=1 - 9.9$). Linear regression on the data gives correlation coefficients $r = 0.98$ for $C_{ABS}-C_{TSS}$ plot under $H_s=0.8, 1.0$ and 1.2 m. As can be seen here, the concentrations is very close to the line $C_{ABS}=C_{TSS}$. For ABS measurements, the regression gradients is $C_{ABS}/C_{TSS}=0.9652$, showing a relatively good agreement with the line $C_{ABS} = C_{TSS}$.

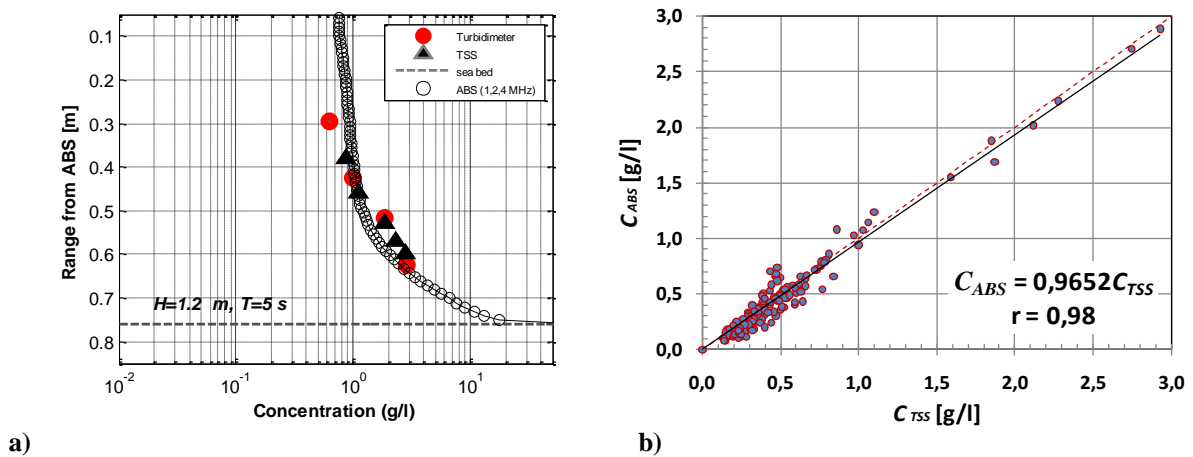


Figure 4: Sediment concentration profiles resulting from different measuring techniques: a) Time- and bed-averaged ABS (closed white circles), Optical Turbidity Meter (closed red circles) and TSS (black triangles) concentrations under regular waves ($H=1.2$ m, $T= 5$ s). b) Regression plots of the mean acoustic concentrations: ABS concentrations against TSS concentrations at 0.14, 0.17, 0.21 and 0.37 m above the sand bed under regular and irregular waves (Test condition: $H_s, H = 0.8, 1.0$ and 1.2 m; $T_p, T = 5$ s and the peak enhancement factor $\gamma = 1 - 9.9$).

4.2 INTRAWAVE ANALYSIS

Figure 5 shows the details of the intrawave induced concentration event occurred over a time period of 450 s (90 successive non breaking regular waves), i. e. as the ripple migrated landwards beneath ABS. Each suspended concentration contour pattern in Figure 5 (panels a to f) shows the suspended concentration entrainment around a step 2D-ripple for different phases depicted on a wave cycle shown in the velocity panel on the top of the Figure 5. Figure 5-a shows the generation of the vortex V1 just after the separation of the positively directed maximum wave induced flow at the crest of the ripple ($t/T \approx 0$). This ripple grows and becomes sediment laden during the rest positive half cycle ($t/T \approx 0.2$) (Figure 5-b). After the first flow reversal ($t/T \approx 0.3$), the vortex V1 separates from the ripple surface (Figure 5-c). Whereas the detached sediment-rich lee vortex, V1, is advected under the reversed negatively directed wave induced flow, the second lee vortex, V2, is formed at the opposite side of the ripple due to the reversed flow and grows during the remaining negative wave half cycle and moves over the ripple crest ($t/T \approx 0.4, 0.6$ and 0.8 , respectively) (Figure 5-d and e). As can clearly be seen here, vortex V2 is smaller than V1 and is not shed significantly, as it was the case by V1, which is the consequence of the wave asymmetry (cf. Figure 2).

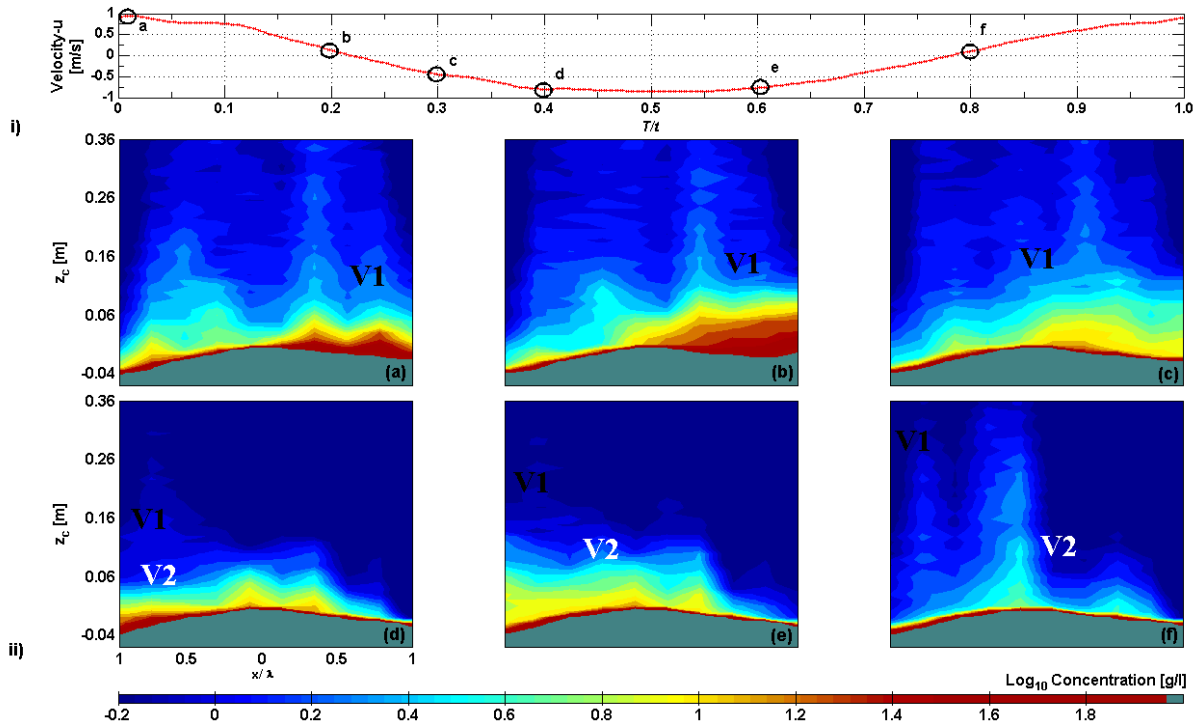


Figure 5 : i) Horizontal component of the wave induced orbital velocity at 6 selected phase angles of the entire wave cycle, ii) Selected sound imaging of vortex generations and suspended sediment entrainment over a ripple under non-breaking regular waves for the depicted phases at the velocity panel (a). V1 indicates the vortex generated at the on-shore flank of the ripple, when the wave induced flow is maximum and positively directed, whereas V2 indicates the vortex generated at the opposite side of the ripple under the negatively directed wave induced flow.

5. CONCLUDING REMARKS

Observations of the intrawave sediment entrainment event induced by regular non-breaking waves show that over steep ripples, the generation of the lee-wake vortices followed by their shedding in the opposite direction are the primary sediment transport processes, which occur twice within each wave cycle. However, in the case of asymmetric non-breaking Stokes waves ($Ur=10-26$), the vortices generated at the on-shore flank of ripple crests are larger than those generated at the offshore flank of the ripple crests under the negatively directed wave induced flow. Due to the fact that the offshore pumping of detached sediment-rich vortices, generated under positively directed flow, during the longer negative cycle of Stokes waves is more significant, the total net transport of suspended sediment concentration above ripples is offshore directed. Moreover, the experiments showed that the steep 2-dimensional ripples migrate during the test runs in the direction of the wave propagation, possibly due to the vertical asymmetry of the waves.

Hence, two sediment transport forms can be recognised above steep vortex ripples under asymmetric non-breaking waves: (i) Seawards suspended sediment transport due to the offshore directed advection of the sediment laden lee vortices. (ii) Shorewards bed load during the onshore directed ripple migration.

More details on the results are given in Ahmari and Oumeraci (2011), including suggested non-dimensional parameters governing wave induced sediment concentration processes and the implications for future modelling when using the diffusion equation.

6. ACKNOWLEDGEMENTS

The experiments are partly supported by the European Community within the Sixth Framework Program as a part of the Joint Research Activity “SANDS”, in the Integrated Infrastructure Initiative HYDRALAB III and partly by the BMBF supported project “ModPro” (03KIS060).

7. REFERENCES

- AHMARI, A.; GRÜNE, J.; OUMERACI, H.: Large scale laboratory measurement of suspended sediment concentration induced by non-breaking waves with acoustic backscatter technique, Proc. on App. of Phy. Mod., Coastlab'08, Bari, Italy, 93-105; 2008.
- AHMARI, A.; GRÜNE, J.; OUMERACI, H.: Zur Messung wellenerzeugter suspendierter Sedimentkonzentrationen 7. FZK-Kolloquium 'Potenziale für die Maritime Wirtschaft', Hannover, 2009.
- AHMARI, A., OUMERACI, H.: Measurement and analysis of the suspended sediment concentration by waves in a rippled bed regime,” 9st Int. Conf. on Coasts, ports and marine structures (ICOPMAS-2010), Teheran, Iran; 2010.
- AHMARI, A., OUMERACI, H.: Comparative analysis of suspended sediment concentration recorded with different techniques in the rippled bed regime. 31st Int. Conf. on Coastal Engineering (ICCE-2010), Shanghai, China, 2010.
- AHMARI, A., OUMERACI, H : Measurement and analysis of near bed sediment transport processes by waves in rippled bed regime. ASCE, Proc. Conf. Coastal Sediments, Miami, Florida, 2011 (submitted)
- BLONDEAUX, P. and VITTORI, G.: Vorticity dynamics in an oscillatory flow over a rippled bed, J. Fluid Mech., 226, 257-289, 1991.
- HANSEN, E. A.; FREDSOE J.; DEIGAARD, R.: Distribution of suspended sediment over wave-generated ripples, J. Waterway, Port, Coastal and Ocean Engineering, 120(1), 37-55, 1994.
- MALARKEY, J. AND DAVIES, A. G., Discrete vortex modelling of oscillatory flow over ripples, Applied Ocean Res., 24(3), 127-145, 2002.
- NIELSEN, P.: Coastal Bottom Boundary Layers and Sediment Transport, Advanced series on Coastal Engineering- Volume 4, World Scientific, 1992.
- RIBBERINK, J.S. and AL-SALEM, A. A.: Sediment transport in oscillatory boundary layers in case of rippled beds and sheet flow, J. Geophys. Res. 99(C6): 12707- 12727, 1994.
- THORNE, P. D.; DAVIES, A. G.; PAUL, S. : Observations and analysis of sediment diffusivity profiles over sandy rippled beds under waves, J. Geophys. Res. Vol. 114 C02023. 1-16, 2009.
- THORNE, P. D.; DAVIES, A. G.; WILLIAMS, J. J.: Measurements of near bed intrawave sediment entrainment above vortex ripples. Geophys. Res. Lett., Vol. 30, No. 20, 2028, OCE, 2-1 - 2-4, 2003.